Engineering Conferences International
ECI Digital Archives

The 14th International Conference on Fluidization
– From Fundamentals to Products

Refereed Proceedings

2013

Fluidisation of Amorphous Granules

Stefan Palzer
Nestec SA, Switzerland

Stefan Heinrich
Hamburg University of Technology, Germany

Follow this and additional works at: http://dc.engconfintl.org/fluidization_xiv

Part of the Chemical Engineering Commons

Recommended Citation

Fluidisation of amorphous granules

- Practical challenges, product structures and progress in modelling -

Stefan Palzer[1], Stefan Heinrich[2]
[1]Nestec SA
AvenueNestlé 55
CH-1800 VEVEY
Stefan.palzer@nestle.com
[2]Institute of Solids Process Engineering and Particle Technology,
Hamburg University of Technology,
Denickestrasse 15, 21073 Hamburg, Germany

ABSTRACT

In many industries amorphous powders are agglomerated and granules are dried in fluid beds. The current contribution discusses issues related to fluid bed processing observed in industrial applications. Fluidization of irregular shaped particles is discussed and published equations for calculating the minimal fluidization velocity are validated for real food granules. Furthermore lumping and bed collapse which are occasionally observed during fluid bed agglomeration of amorphous water soluble powders is investigated. Temperature and moisture conditions leading to such undesired agglomeration effects are defined based on changing material properties. Finally the state of the art in modeling of fluidized bed systems is briefly described.

INTRODUCTION

Most food products and food ingredients, detergents, many fine chemicals and pharmaceutical products comprise of amorphous granules. Such granules are typically produced by drying, agglomeration or wet granulation. Commonly these processes involve a drying and a subsequent cooling step which are most often performed in fluidised beds. During drying and cooling of granules heat and mass transfer can be improved by mechanical or pneumatically fluidisation of the product. In addition adhesion forces between particles are limited in fluid beds due to the acting shear forces and the comparable short contact time.

Particles can be fluidised mechanically by rotation of a drum or pan containing the product or by stirring those using fast rotating tools. Alternatively pneumatical fluidisation of particles can be achieved by exposing them to a vertical air stream which compensates gravity. In fluid bed agglomeration and coating processes commonly aqueous liquid solutions are sprayed on these moving particles.

The current contribution will focus on pneumatically fluidised beds. We will evaluate how far it is possible to predict fluidisation conditions for irregular shaped particles in industrial applications. We will also elaborate why frequently lumping or even collapse of the fluid bed is observed while atomising aqueous solutions on the moving particles. Such phenomena will be explained through the changing properties of the amorphous material. Furthermore we will also discuss the structural characteristics of amorphous granules manufactured in fluidised

beds. Finally the state of the art in modelling such processes is presented and the importance of material properties in ensuring applicability of models is highlighted.

CHALLENGES IN FLUID BED AGGLOMERATION OF AMORPHOUS POWDERS

Major challenges for predicting optimal process parameters for fluidisation are the non-spherical particle shape, the influence of the particle size distribution and the temperature and moisture dependency of adhesion forces.

For modelling the behaviour of a fluidised bed of granules the pressure loss of the bed has to be estimated. Ergun [1952] calculated the pressure loss caused by a layer of spherical particles. Introducing the mean Sauter diameter d_p and the sphericity φ (ratio between surface area of a volume equivalent sphere to the surface area of the particle) the pressure loss of a bed of irregular-shaped particles can be estimated through equation (1) [Uhlemann and Mörl, 2000]:

$$\Delta p = h \cdot \left(150 \cdot \frac{(1-\varepsilon)^2}{\varepsilon^3} \cdot \frac{\eta_a \cdot u}{(\varphi \cdot d_p)^2} + 1.75 \cdot \frac{1-\varepsilon}{\varepsilon^3} \cdot \frac{\rho_a \cdot u^2}{\varphi \cdot d_p^2} \right) \quad with \; S_v = \frac{6}{\varphi \cdot d_p} \tag{1}$$

S_v is the specific surface area of the powder and ε represents the bed porosity. ρ_a is the symbol used for the density of the fluidisation air while η_a stands for the air viscosity. u represents the minimal air velocity required to loosen a package of cohesionless particles and to initiate fluidisation. h symbolise the height of the powder bed.

Setting the pressure difference required for separating particles from each other equal to the pressure loss caused by friction between air and the irregular shaped particles, the minimal air velocity u required for fluidisation of the powder can be calculated for the laminar (Re<1) and for the turbulent (Re>1000) flow regime through equations (2) and (3) [Uhlemann and Mörl, 2000].

$$u = \frac{1}{150} \cdot \frac{\varepsilon^3}{1-\varepsilon} \cdot \frac{g \cdot (\varphi \cdot d_p)^2}{\eta_a \cdot \rho_a} \cdot (\rho_s - \rho_a) \quad for \; Re = \frac{u \cdot d_p \cdot \rho_a}{\eta_a} \leq 1 \tag{2}$$

$$u = \sqrt{\frac{1}{1.75} \cdot \varepsilon^3 \cdot g \cdot \varphi \cdot d_p \cdot \left(\frac{\rho_s - \rho_a}{\rho_a} \right)} \quad for \; Re = \frac{u \cdot d_p \cdot \rho_a}{\eta_a} \geq 1000 \tag{3}$$

Re is the dimensionless Reynolds number. ρ_s represents the density of the particles.

Fig. 1 shows a fluidised bed of large agglomerates at incipient fluidisation (left side) and a bubbling fluid bed of the same agglomerates (right side). Incipient flow should be reached once the air velocity reaches u. Bubbling fluidisation is achieved if the fluidisation velocity is significantly larger then u but still smaller then the velocity leading to pneumatical conveying of the particles.

Fig. 1: Different fluidisation states in a continuously operated fluid bed. Left: incipient/minimum fluidisation; Right: bubbling or aggregative fluidisation

However, it has to be evaluated if equations (2) and (3) deliver realistic air velocity values for real particle systems with irregular shaped particles. Following we performed calculations of the theoretical minimal fluidisation velocity $u_{cal.}$ for three very different amorphous food powders and compared them with measured fluidisation velocities for these 3 product systems. The experimental air velocity u_{exp} was estimated based on fluidisation trials and qualitative optical assessments according to the photos shown in Fig. 1.

Fig. 2 shows the 3 different food powders and the table below includes measured minimal air velocities $u_{exp.}$ required for their fluidisation as well as the minimal air velocity $u_{calc.}$ calculated according to equation *(2)* or *(3)*.
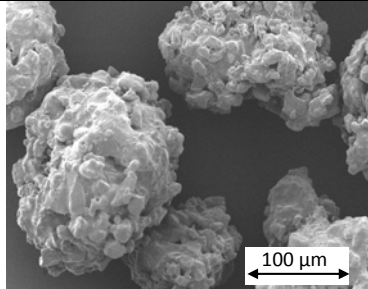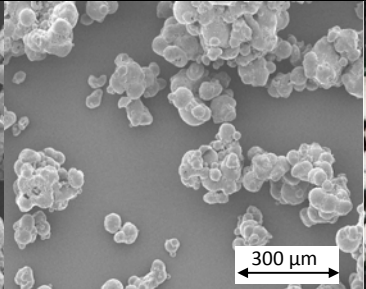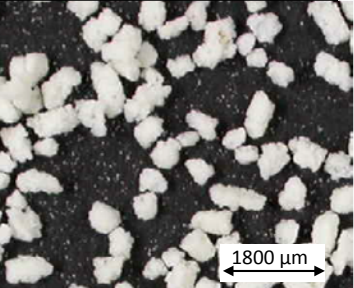

Agglomerated beverage powder	Spray-dried skim milk powder	Extruded food agglomerates
ε=0.6; d_p=0.002 m; Re=170	ε=0.6; d_p=0.0003 m; Re=5	ε=0.5; d_p =0.0016 m; Re=55
ρ_s=1000 kg/m³; ρ_a=0.9 kg/m³	ρ_s=1200 kg/m³; ρ_a=0.9 kg/m³	ρ_s=1800 kg/m³; ρ_a=0.9 kg/m³
$u_{exp.}$ = 1.10 m/s	$u_{exp.}$ = 0.29 m/s	$u_{exp.}$ = 0.7 m/s
$u_{calc.}$ = 1.64 m/s (equ. turb.)	$u_{calc.}$ = 0.31 m/s (equ. lam.)	$u_{calc.}$ = 1.5 m/s (equ. turb.)

Fig. 2: Comparison between the calculated minimal air velocity $u_{calc.}$ and the experimentally determined minimal air velocity $u_{exp.}$ required for fluidisation

The calculated and experimentally determined minimal air velocities are in the same order of magnitude. Only for the rod shaped extruded agglomerates (right image) a significant difference between the calculated and experimental air velocity is observed. Apparently the equations (2) and (3) are useful to estimate the minimal air velocity required for fluidisation of irregular shaped granules with limited adhesion forces between them. For fluidisation of food products an air

velocity between 0.2 and 2 m/s is typically applied [Palzer, 2007]. Vibration of the equipment frame enables to operate the bed at the lower end of this velocity range [Pisecký, 1997].

A major challenge experienced in fluid bed processing of amorphous granules is the often observed lumping and collapse of the bed. Equations *(2)* to *(3)* are valid only for granules with small inter-particle adhesion forces. In agglomeration of powders in fluid beds often water or a water-based binder solution is atomised on fluidised particles. Thus, the relative humidity of the fluidising air surrounding the particles and the water content of the particle surface increase with increasing spraying time. Furthermore the viscosity of amorphous water soluble materials strongly depends on the water content. Absorbed water acts as plasticiser decreasing the glass transition temperature and the viscosity of the material as described in earlier publications [Palzer, 2010]. Since the amorphous material behaves visco-elastic its mechanical properties are either characterised through the storage and loss modulus or the complex modulus which is a combination of both. Alternatively mechanical properties can be described via the complex and/or the zero shear viscosity. The complex viscosity and the zero shear viscosity η_0 of the amorphous material are a function of temperature T and glass transition temperature T_G [Palzer, 2009; Palzer, 2010]:

$$\eta_0(T) = \eta_0(T_G) \cdot a_T \qquad with \ a_T = 10^{\frac{-C \cdot (T-T_G)}{B+(T-T_G)}}$$

(7)

a_T is the constant shift factor to be applied in the frame of the superposition principle to calculate the viscosity based on the viscosity at a reference temperature (in thi s case the glass transition temperature). The glass transition temperature itself is a function of the water content [Palzer, 2009].

With increasing humidity of the air in the system the surface viscosity of amorphous particles thus decreases. The decreasing surface viscosity supports the development of adhesion forces in form of viscous bridges between colliding amorphous particles. These bridges are formed by initial plastic deformation as a result of particle collisions and following rapid sintering. If the velocity of the fluidising air is kept constant, the shear forces exerted by the air stream might not be sufficient to separate colliding particles from each other. The pressure loss of the fluid bed increases due to the increasing adhesion forces between the particles and thus can be used as an indicator for an imminent collapse of the fluid bed. Such a collapse of the bed starts in zones of the agglomerator where the turbulence is reduced and, thus, the particles are exposed to a lower shear stress. Large lumps are formed and gradually the amount of caked powder, which is attached to the equipment surface, grows. Due to an increasing pressure loss the air velocity decreases leading to a reduction of the shear stress in the bed. Finally, the entire bed collapses, which means all particles form a single, large sintered powder package. Once the bed has collapsed, it is difficult to re-fluidise it again due to steadily increasing adhesion forces between particles caused by ongoing sintering processes. To prevent such a collapse of the bed it is required to adjust the air velocity during the binder injection to compensate for the increasing adhesion forces. Increasing the air velocity reduces the time available for building bridges between the particles and increases the shear stress on established bridges by increasing the mean particle velocity. In addition, the density of the fluid bed is reduced. Hence, the probability of collisions between particles also decreases. Another possibility to prevent the described collapse of the fluid bed is to limit the increase in relative humidity of

the air by reducing the flow rate of the aqueous binder. Furthermore increasing air temperature and velocity will also help to avoid such moisture induced collapse by removing increasing amount of water from the bed.

To predict the collapse of the bed it is required to investigate the adhesion forces between the fluidised amorphous particles. These forces are strongly linked to the material properties which are for amorphous water-soluble substances a function of temperature and water content. The knowledge of the moisture content of the particle surface enables to calculate the corresponding glass transition temperature of the material. The obtained difference between product and glass transition temperature $T-T_g$ can be used to estimate the surface viscosity and thus the risk of a collapse of the fluid bed. It can be expected that at viscosities between 10^6-10^8 Pas strong adhesion forces develop [Palzer, 2005; Palzer, 2007].

In the current study the agglomeration of amorphous dextrose syrup (DE21), spray-dried skim milk powder (<1% fat) and spray-dried whole milk powder (20-25% fat) in a batch-wise operated fluid bed was investigated. Fig. 3 and 4 show moisture/temperature combinations obtained during the agglomeration of all three powders. In order to be able to compare both milk powder types the water content was based on non-fat solids (SNF). The moisture content depicted in figures 2 and 3 represents the water content on the particle surface. It is obtained by measuring the relative humidity of the exhaust air and transforming the obtained values into the corresponding water contents using the products sorption isotherm. The open symbol represents temperature/moisture combinations of a classical agglomeration process. The curves included in Fig. 3 and 4 represents the glass transition temperature of dextrose syrup (Fig. 3) and lactose (Fig. 4) which was calculated as published earlier [Palzer, 2005].
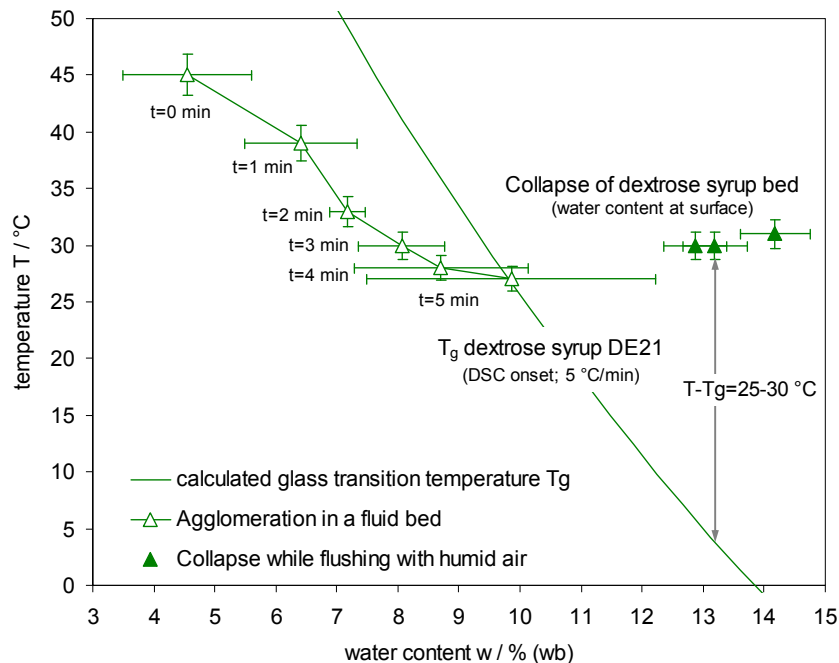

Fig. 3: Temperature/moisture combinations during agglomeration of dextrose syrup (DE 21) in a batch-wise operated fluid bed (Glatt GCPG 3.1; liquid throughput 40 ml/min)
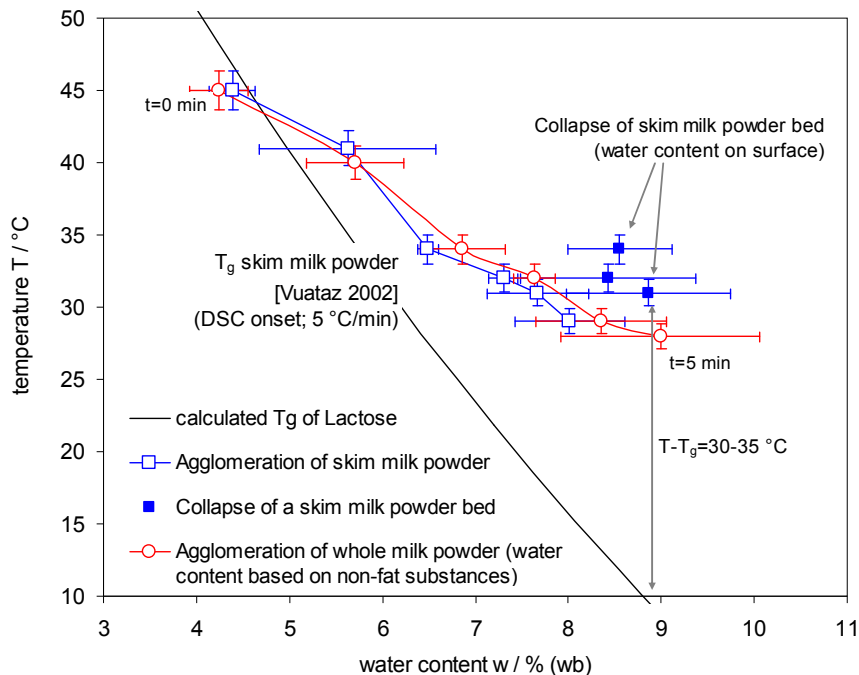
Fig. 4: Temperature/moisture combinations during agglomeration of skim and whole milk powder in a fluid bed (Glatt GPCG 3.1; water content calculated using r.H. of air in the bed)

With progressing agglomeration time and an increasing amount of atomised water the relative humidity of the air in the bed increases while the particle temperature decreases due to the evaporation of water.

After 5 minutes agglomeration time the injection of water is terminated. At this point the temperature of the Dextrose syrup particles is in the same order of magnitude than the glass transition temperature at the humid particle surface. Under such conditions the viscosity of the amorphous matrix is still in the order of 10^{10} to 10^{12} Pa·s [Palzer, 2005; Palzer, 2007] and, thus, the particles would require a comparably long contact time to adhere to each other due to the development of sinter bridges. Accordingly, sinter bridges can only be built on surface areas which are wetted by impacting water droplets. At this stage the liquid injection is terminated and the agglomerated powder is dried and cooled to provide a shelf-stable product. A comparable low content of oversize particles is obtained and no collapse of the bed is observed.

Maintaining the same spray rate, the humidity of the non-fat substance of the dairy powders increases faster because the same injected water amount is absorbed by a reduced amount of water soluble amorphous substance (which is in case of the milk powders mainly Lactose). The humidity of the whole milk powder increases even faster than the one of skim milk powder due to the reduced amount of non-fat solids. The injected water amount is absorbed entirely by the reduced amount of amorphous Lactose. However, all three powders behave similar during agglomeration in terms of moisture absorption.

Agglomerating or coating amorphous water soluble particles in fluid beds often a collapse of the bed is observed. In the current study conditions leading to such

collapse were investigated. Following earlier studies stickiness of non moving particles is observed at temperature difference T-Tg exceeding 15-20 ºC [Palzer, 2005]. At such conditions the surface viscosity is around 10^6-10^8 Pas. Accordingly, the risk of a collapse of the powder bed is comparably high. To measure the conditions at which a collapse of the fluid bed consisting of moving particles can be expected the powder bed was exposed to humid air with varying humidity streaming through the bed. When the moisture content or the temperature of the air is further increased, a sudden collapse of the fluid bed can be observed. The closed symbols in Fig. 3 and 4 represent process conditions leading to such a collapse of the entire fluid bed. In our studies for all three powders such a collapse of the fluid bed was observed at 25 to 35 °C difference between the product and the glass transition temperature. At these conditions we can assume a strong plasticisation of the entire particle surface due to an increasing humidity of the air inside the fluid bed. This conclusion is valid for all three amorphous powders used. For the two milk powders the conditions at the end of the 5 minute agglomeration cycle are close to the collapse conditions and accordingly a larger number of oversize particles are obtained.

Fig. 5 shows scanning electron microscope pictures of a collapsed dextrose syrup powder bed. The smooth particle contours clearly indicate that the entire surface of all particles is plasticised by the moisture absorbed from the surrounding air.
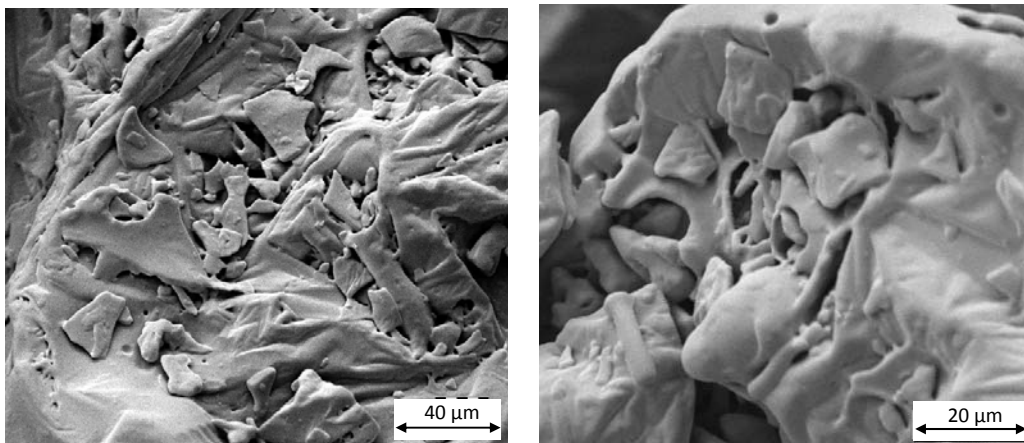

Fig. 5: Images of a collapsed dextrose syrup (DE 21) powder bed (SEM pictures; agglomeration in a Glatt GCPG 3.1)

To avoid temperature/moisture combinations leading to such collapse, the aqueous binder has to be atomised with a low spray-rate onto the fluidised particles allowing the current of air to convey the evaporated moisture out of the fluid bed. Alternatively, the total added binder quantity can be reduced. In both cases the final   relative humidity of the air inside the fluid bed decreases and, hence, the glass transition temperature T_g and the viscosity of the particle surface increases.

In summary it can be concluded that during agglomeration of amorphous powders the glass transition temperature of the amorphous component at the particle surface (e.g. Dextrose or Lactose) should not be exceeded by more than 25 °C in order to avoid a collapse of the fluid bed.

Such collapse of a bed of amorphous particles is also observed in mechanical fluidisation of granules in mixers if water or aqueous solutions are atomised on the moving particles too rapidly or mechanical fluidisation is performed at high relative humidity. As in pneumatical fluidisation, amorphous material at the particle surface absorbs water and thus gets plastified. Accordingly, plastic deformation of the outer particle regions upon collisions is facilitated and rapid sinter processes are enabled. Due to the action of mixing tools no large cake is obtained and a bed collapse is less obvious. However, large porous and friable lumps are formed. Such lumping is observed at similar T-Tg conditions as in pneumatically fluidised beds.
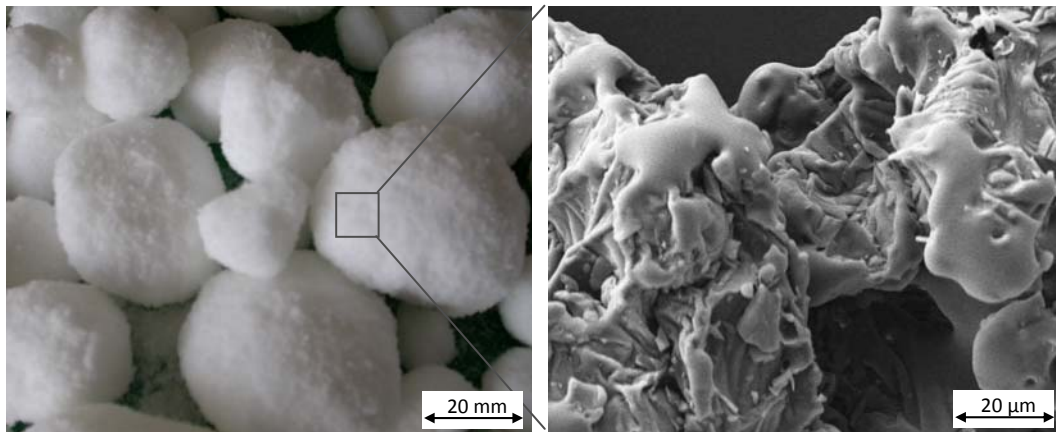

Fig. 6: Dextrose syrup (DE 21) lumps obtained by mixing the powder in a ploughshare mixer at T-T_G >25 ºC (left: light microscopic picture; right: SEM image)

Assuming that sintering is responsible for the observed undesired agglomeration during fluid bed processing of amorphous powders, it should be possible to estimate the risk of lumping through equations describing the kinetics of sintering and plastification. Sintering is a time-dependent process and the contact time between the particles has to be known in order to calculate the sinter bridge diameter. However, it remains difficult to estimate the contact time between colliding particles in pneumatically or mechanically fluidised beds. Modelling remains the only possibility to estimate theoretically conditions leading to lumping and bed collapse. In addition, it is difficult to measure the water activity on the particle surface which in turn determines the viscosity in mixers. Either the relative humidity of the air inside the fluid bed or mixer is measured or the water activity of the powder is analysed off-line shortly after the process.

STRUCTURAL CHARACTERISTICS OF AMORPHOUS AGGLOMERATES PRODUCED IN FLUIDISED BEDS

During agglomeration of amorphous powders and drying of amorphous granules in fluid beds it remains difficult to provide a narrow particle size distribution and to avoid the generation of oversize particles. In fluid bed agglomeration water or aqueous binder droplets are impacting on amorphous particle surfaces. The moisture is absorbed by the hydrophilic surface material generating a viscous solution. Particles impacting on this solution are adhering with a high probability due to effective energy dissipation by viscous forces and the generation of a

viscous bridge between the two particles. Thus growth is often rather random and shear forces in the bed are not able to generate spherical particles by abrasion. Therefore frequently random shaped particles are obtained. If liquid binder is finely atomised on the bed and binder flow rate is rather low more spherical particles are obtained. Generally, the produced agglomerates possess a rather low density. The size of agglomerates produced in fluid beds strongly depends on the shear forces within the moving powder bulk. $d_{50,3}$ values between 0.3 and 10 mm are possible. Recirculation of fines leaving the system with the exhaust air produces grape like structures by agglomeration with moist particles.

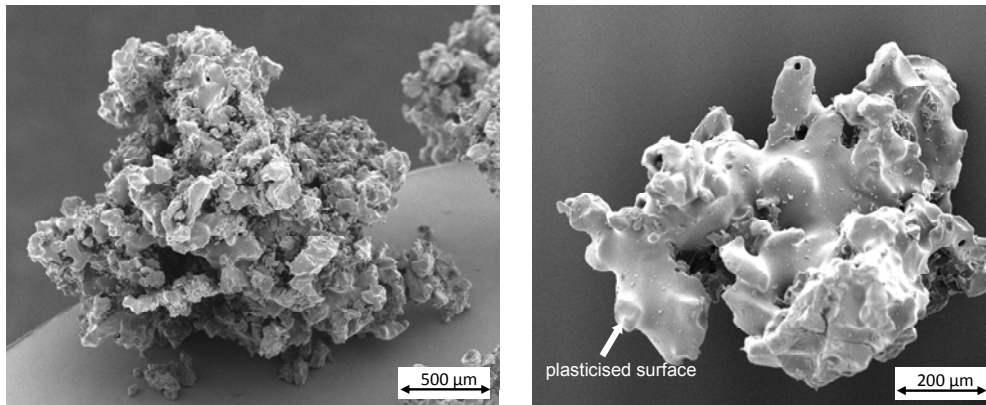Fig. 7, Fig. 8 and Fig. 9 show particles obtained by fluid bed agglomeration.

Fig. 7: Dextrose syrup (DE 21) agglomerates produced in a batch-wise operated fluid bed (SEM pictures; agglomerator Glatt GCPG 3.1, Glatt GmbH Binzen/G)
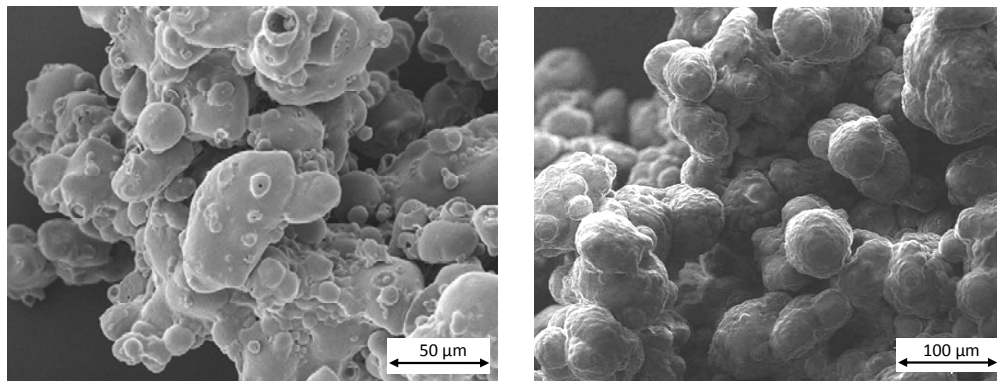

Fig. 8: Skim milk (left) and whole milk (right) powder agglomerated in a batch-wise operated fluid bed (SEM images)
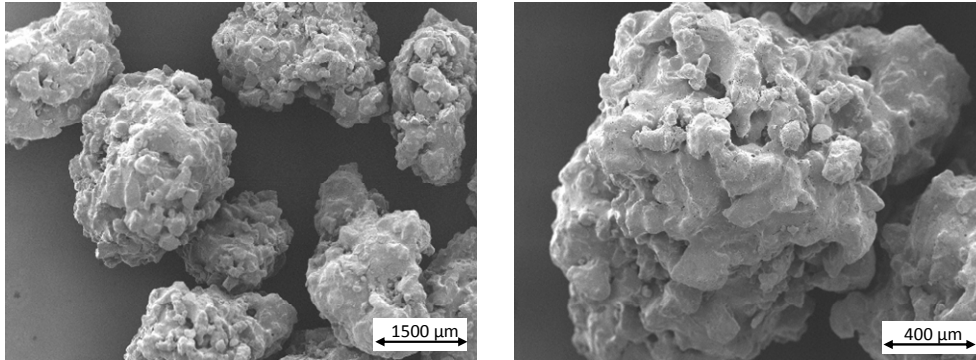
Fig. 9: Amorphous food powder agglomerates produced in a continuous fluid bed agglomerator

STATE OF THE ART IN MODELLING FLUID BED AGGLOMERATION OF AMORPHOUS WATER SOLUBLE PARTICLES

Modelling fluid bed agglomeration of water soluble particles is required to identify favourable agglomeration conditions delivering the desired narrow particle size distribution and avoiding collapse of the bed. One of the major problems in modelling fluid bed agglomeration was that the majority of models were developed under the assumption of inert and often also ideally spherical monodisperse particles. Material properties were often neglected. Thus models were lacking industrial applicability and relevance. However, in the past years work in the area of adhesion forces and their dependency on the material properties has been performed [Haider et al., 2012; Fries, 2012]. This resulted in the development of more realistic micro-models.

The main remaining problem of numerical modelling of such agglomeration processes is a gap between the scales, where detailed models, based on the material micro properties, exist and the production scale, as the point of interest for practical application [Werther et al., 2011]. The major number of industrial studies is based on the process modelling with usage of empirical or semi-empirical models, which represent a possibility to obtain a solution in acceptable time. However, empirical models have a limited accuracy level and relative small parameter space, where they can be effectively used. To increase the accuracy of the process description, sub-models which are relevant at different time and length scales can be combined by interscale communications into one multiscale model [Dosta et al., 2012].

Nowadays, the population balance models (PBM) can be effectively used for the description of the process on the macroscale. The implementation of these models into flow sheet simulation systems allows investigating the behaviour of production processes [Dosta, 2013]. The parameters for the PBM can be approximated from the lower scales of the process description. The material micro parameters can be precisely described by the discrete element method (DEM), where each particle is considered as a separate entity. The motion of the particles is calculated using Newton's second law:

$$m\frac{d^2r}{dt^2} = F_D + F_G + \sum_{i=1}^{N_{cp}} F_{cp,i} + \sum_{i=1}^{N_{cw}} F_{cw,i}, \tag{5}$$

F_D and F_G are drag and gravity forces, respectively. $F_{cp,i}$ and $F_{cw,i}$ represent forces caused by contact with other particles and apparatus walls.

In a fluidized bed (FB) process also the gas flow plays an important role. Therefore, the DEM system is coupled with a Computational Fluid Dynamics (CFD) model to obtain the fluid profile in the apparatus. For the CFD calculation of the fluid phase, the apparatus is discretized into mesh cells. For each cell the gas flow field is described using the volume-averaged Navier-Stokes equations:

$$\frac{\partial}{\partial t}\left(\varepsilon\rho_g\right) + \nabla \cdot \left(\varepsilon\rho_g\mathbf{u}_g\right) = 0 \tag{6}$$

$$\frac{\partial}{\partial t}\left(\varepsilon\rho_g\mathbf{u}_g\right) + \nabla \cdot \left(\varepsilon\rho_g\mathbf{u}_g\mathbf{u}_g\right) = -\varepsilon\nabla p_g - \nabla \cdot \left(\varepsilon\boldsymbol{\tau}_g\right) - \mathbf{S}_p + \varepsilon\rho_g\mathbf{g} \tag{7}$$

In this context τ_g is the gas phase stress tensor.

To describe the interactions between colliding particles contact models are used. Different contact scenarios between dry particles, wetted particles and between particles and droplets have to be taken into account. Correlations, based on a critical Weber number [Bai, 2002] are used to describe the droplet deposition on the particles in the fluidized bed (Fig 10).
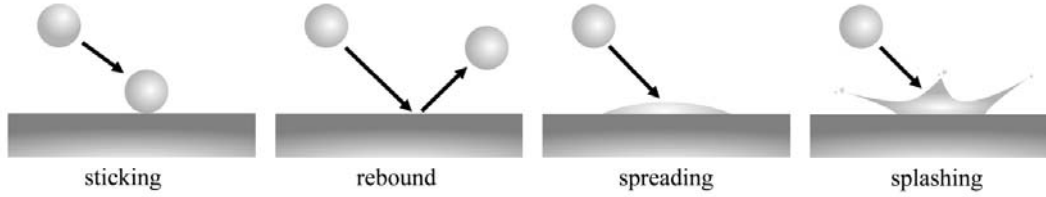

sticking   rebound   spreading   splashing

Fig. 10: Droplet impact scenarios according to [Panao, 2004]

$$We = \frac{\rho_d \cdot u^2 \cdot d_d}{\sigma_d} \tag{8}$$

Based on the critical Weber numbers and the material properties critical collision velocities between particles and droplets can be calculated that decide if the particle is wetted or not:

$$u_{crit} = \sqrt{\frac{We_{crit} \cdot \sigma_d}{\rho_d \cdot d_d}} \tag{9}$$

Droplets are considered as discrete elements that collide with particles and their mass is transferred to the particle depending on the collision velocity that is calculated in the DEM model.

For the agglomeration of amorphous particles the energy during the collision of two or more particles has to be dissipated due to viscous and capillary forces of the liquid layer on the wetted particles surfaces (Fig. 11).

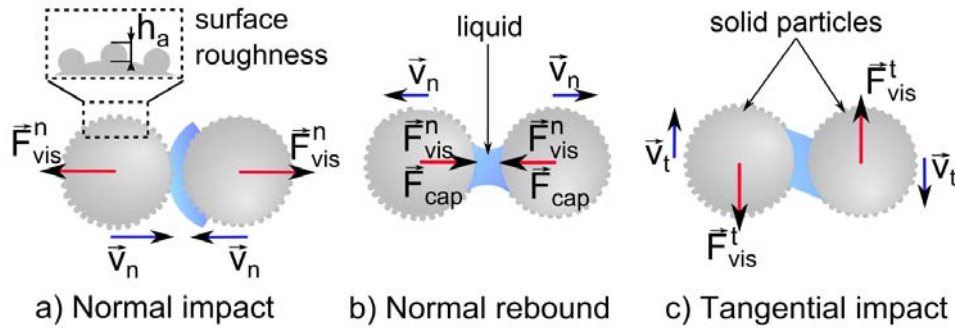a) Normal impact   b) Normal rebound   c) Tangential impact

Fig. 11: Different types of impact of wetted particles

The normal and the tangential components of the viscous force are calculated using Eqs. (10) and (11), respectively [Adams, 1987; Popov, 2010].

$$F_{vis}^n = \frac{6 \cdot \pi \cdot \eta \cdot \bar{R}^2 \cdot v_{n,rel}}{L} \qquad (10)$$

$$F_{vis}^t = 2 \cdot \pi \cdot \eta \cdot \bar{R} \cdot v_{t,rel} \cdot \ln\left(1 + \frac{\bar{R}}{2L}\right) \qquad (11)$$

$$\bar{R} = R_1 \cdot R_2/(R_1 + R_2) \qquad (12)$$

R_1 and R_2 are the radii of the contact partners. $v_{n,rel}$ and $v_{t,rel}$ describe the normal and tangential components of the relative impact velocity. η is the liquid viscosity. The distance between the particle surfaces L is limited by the minimum value of L=2ha, where h_a is the particle roughness.
Capillary forces depend on the surface tension σ of the liquid, the volume of the bridge V and the contact angel between the solid and the fluid and are calculated using the model of Pitois et al. [Pitois, 2000]:

$$F_{cap} = 2 \cdot \pi \cdot \bar{R} \cdot \sigma \cdot cos\theta \cdot \left(1 - \left(1 + \frac{2 \cdot V}{\pi \cdot \bar{R} \cdot L^2}\right)^{-0.5}\right) \qquad (13)$$

In the future these models will be combined with equations describing mechanical material properties as a function of temperature and water content and as well the distribution of these parameters within single particles.

REFERENCES

Adams, M.; Edmondson, B. (1987): Tribology in Particulate Technology (Eds. B.J. Briscoe, M.J. Adams), Adam Hilger, Bristol

Bai , C.; Rusche , H.; Gosman, A. (2002): Atomization Sprays 12 (1-3). pp. 1-27

Dosta, M. (2013): Dynamic flowsheet simulation of solids processes and its application to fluidized bed spray granulation. Cuvillier Verl., Göttingen. pp. 142

Dosta, M.; Antonyuk, S.; Heinrich, S. (2012): Multiscale simulation of fluidized bed granulation process. Chemical Engineering and Technology 35 (8). pp. 1373-1380

Ergun, S. (1952): Fluid flow through packed columns. Chemical Engineering Progress 48, pp. 89-94

Fries, L. (2012): Discrete particle modeling of a fluidized bed granulator. PhD thesis. Institute of Solids Process Engineering and Particle Technology. Technical Universitry of Hamburg Harburg. Curvillier Verlag Goettingen

Haider, C.; Althaus, T.; Niederreiter, G.; Hounslow, M.; Palzer, S.; Salman, A. (2013): A micromanipulation particle tester for agglomeration contact mechanism studies in a controlled environment. Measurement Science and Technology 23 (10). pp. 12. Article already online under 105904

Palzer, S. (2000): Anreichern und Benetzen von pulverförmigen Lebensmitteln mit Flüssigkeiten in diskontinuierlichen Mischaggregaten. PhD thesis. Chair for Process Engineering of Disperse Systems. Technical University of Munich. Munich/G.

Palzer, S. (2005): The effect of glass transition on the desired and undesired agglomeration of amorphous food powders. Chemical Engineering Science 60 (14). pp. 3959-3968.

Palzer, S. (2009): Influence of material properties on the agglomeration of water-soluble amorphous particles. Powder Technology. 189. pp. 318-326

Palzer, S. (2010): Relating the supra-molecular structure of water-soluble food solids with their material properties. Trends in Food Science and Technology 21 (1). pp. 12-25

Palzer, S. (2011): Similarities in the agglomeration of pharmaceuticals, detergents, chemicals and food powders -Similarities and differences of materials and processes-. Powder Technology 206 (1-2). pp. 2-17

Panao, M.; Moreira, A. (2004): Exp. Fluids 37 (6) pp. 834-855

Písecký, J. (1997): Handbook of milk powder manufacture. Niro A/S, Copenhagen/DK

Pitois, O.; Moucheront, P.; Chateau, X. (2000): J. of Colloid and Interface Science 231. pp. 26-31

Popov, V. (2010): Contact Mechanics and Friction: Physical Principles and Applications. 1st ed., Springer, Berlin Heidelberg

Uhlemann, H.; Mörl, L. (2000): Wirbelschicht Sprühgranulation. Springer Verlag, Berlin/G

Werther J., Heinrich S., Dosta M., Hartge E.-U. (2011): The ultimate goal of modeling - simulation of system and plant performance. Particuology 9. pp. 320-329

KEY WORDS
Fluid bed, Agglomeration, Bed collapse, Fluidization velocity, Granules, Modelling